American Journal of Pathology, Vol. 165, No. 6, December 2004


*Vascular Biology, Atherosclerosis and Endothelium Biology*

# Hypoxia in Renal Disease with Proteinuria and/or Glomerular Hypertension

Tetsuhiro Tanaka,* Toshio Miyata,† Reiko Inagi,† Toshiro Fujita,* and Masaomi Nangaku*

*From the Division of Nephrology and Endocrinology,* University of Tokyo School of Medicine, Tokyo; and Molecular and Cellular Nephrology, and Department of Internal Medicine,† Institute of Medical Sciences, Tokai University School of Medicine, Kanagawa, Japan*

**Despite the increasing need to identify and quantify tissue oxygenation at the cellular level, relatively few methods have been available. In this study, we developed a new hypoxia-responsive reporter vector using a hypoxia-responsive element of the 5′ vascular endothelial growth factor untranslated region and generated a novel hypoxia-sensing transgenic rat. We then applied this animal model to the detection of tubulointerstitial hypoxia in the diseased kidney. With this model, we were able to identify diffuse cortical hypoxia in the puromycin aminonucleoside-induced nephrotic syndrome and focal and segmental hypoxia in the remnant kidney model. Expression of the hypoxia-responsive transgene increased throughout the observation period, reaching 2.2-fold at 2 weeks in the puromycin aminonucleoside model and 2.6-fold at 4 weeks in the remnant kidney model, whereas that of vascular endothelial growth factor showed a mild decrease, reflecting distinct behaviors of the two genes. The degree of hypoxia showed a positive correlation with microscopic tubulointerstitial injury in both models. Finally, we identified the localization of proliferating cell nuclear antigen-positive, ED-1-positive, and terminal dUTP nick-end labeled-positive cells in the hypoxic cortical area in the remnant kidney model. We propose here a possible pathological tie between chronic tubulointerstitial hypoxia and progressive glomerular diseases. *(Am J Pathol 2004, 165:1979–1992)***

Mammals possess a number of adaptive mechanisms to cope with a low internal oxygen milieu. On a molecular basis, hypoxia induces erythropoietin (Epo), vascular endothelial growth factor (VEGF), and glycolytic enzymes at the transcription level to compensate for the reduced oxygen and nutrient supply. Hypoxia-inducible factor-1 (HIF-1), which regulates the expression of such genes as Epo, VEGF, and glycolytic enzymes, is clearly one of the most important factors in the cellular response to hypoxia. HIF-1 is a heterodimer composed of $\alpha$ and $\beta$ subunits. It is a member of the basic helix-loop-helix (bHLH) superfamily, which is ubiquitously expressed[1] and rapidly degraded by ubiquitin-proteasome systems in normoxia. Under hypoxic conditions, however, HIF-1$\alpha$ escapes degradation and binds to the constitutively expressed HIF-1$\beta$, also known as aryl hydrocarbon receptor nuclear translocator (ARNT), and exerts its hypoxic response through binding to the *cis*-consensus HIF-1-binding site, the hypoxia-responsive element (HRE).[2–4] Recent studies have provided more solid evidence for the conditional expression of HIF-1 in hypoxia. In normoxia, HIF-1$\alpha$ is enzymatically hydroxylated on conserved prolyl residues in the oxygen-dependent degradation domain, which enables the von Hippel-Lindau protein (pVHL) to bind to HIF-1$\alpha$, culminating in polyubiquitination and degradation.[5–7] Thus, HIF-$\alpha$-mediated transcription is controlled in a highly hypoxia-dependent, specific manner. More importantly, a number of studies have indicated the possibility of using HRE in cancer gene therapy as a selective enhancer under which the expression of various therapeutic substances is increased in hypoxia.[8–11] Likewise, it may well be speculated that the use of HRE in the enhancer region of the reporter vector should enable the development of new hypoxia-sensing markers as well.

Despite the increasing demand for methods to identify and quantify hypoxic cells *in vivo*, tools for detecting low oxygenation status within the tissue have been generally restricted to chemical tools. Among those with potential diagnostic, therapeutic, and research availabilities are 2-nitroimidazoles, such as pimonidazole. They have been shown to bind to hypoxic but still viable cells with an oxygen content of less than 10 mmHg[12] and are used extensively in the field of oncology.

Accepted for publication August 19, 2004.

Address reprint requests to Dr. Masaomi Nangaku, Division of Nephrology and Endocrinology, University of Tokyo School of Medicine, 7-3-1, Hongo, Bunkyo-ku, Tokyo, Japan. E-mail: mnangaku-tky@umin.ac.jp.

In this study, we took advantage of HRE of the rat VEGF gene,[13] developed a novel hypoxia-responsive vector, and constructed a transgenic rat carrying the HRE-driven tagged luciferase gene. With these rats, we challenged the hypothesis that tubulointerstitial hypoxia occurs in the kidney during renal disease and modifies the pathogenic progression using two distinct disease models, puromycin aminonucleoside (PAN)-induced proteinuric renal disease and subtotally nephrectomized glomerular hypertension. For more than a decade it has been proposed that chronic hypoxia, along with proteinuria, contributes greatly to tubulointerstitial injury, a hallmark of progressive renal disease.[14,15] Attractive though this scenario appears,[16,17] the limitations of current methodologies have hampered conclusive observation of renal tubulointerstitial hypoxia, and novel techniques have been eagerly sought.

## Materials and Methods

### Cell Culture and Construction of Hypoxic Environment

The immortalized rat proximal tubular cell (IRPTC) is a cultured cell line derived from proximal tubular cells of 4-week-old male Wistar rats, immortalized by transformation with origin-defective SV40 DNA (generously provided by Dr. Julie R. Ingelfunger, Massachusetts General Hospital, MA, USA).[18] Cells of this line were cultured in Dulbecco's modified Eagle's medium (Nissui, Tokyo, Japan) buffered with 25 mmol/L HEPES (Sigma, St. Louis, MO) at pH 7.4, supplemented with 5% fetal bovine serum (JRH Biosciences, Lenexa, KS), 100 U/ml penicillin, 100 $\mu$g/ml streptomycin, and 0.01 mmol/L nonessential amino acids at 37°C under a humidified atmosphere of 5% $CO_2$/95% air. Hypoxia was induced by exposure to 1 to 10% $O_2$/5% $CO_2$ with the balance as nitrogen in a multigas incubator, APM-30D (ASTEC, Fukuoka, Japan).

### Development of the Hypoxia-Responsive Reporter Vector (Transgene Construction)

To construct an optimal vector that responds maximally in a hypoxic milieu, we constructed a series of luciferase reporter vectors by incorporating varied tandem repeats of HREs and a human minimal CMV promoter (hmCMVp)[19] into the pGL3-basic plasmid (Promega, Madison, WI), namely pHRE ×0, 1, 3, 5, 7-Luc. Complementary oligonucleotides containing a HRE and *Nhe*I recognition sites at both ends (5′-CTAGCCCACAGTGCATACGTGGGCTTCCACAGGTCGTCTG-3′ and 5′-CTAGCAGACGACCTGTGGAAGCCCACGTATGCACTGTGGG-3′) were synthesized, annealed, and cloned into pGL3-basic at *Nhe*I through *Bgl*II sites in tandem repeats, directly or via blunt-ended ligation. A synthetic fragment composed of hmCMVp was inserted at the *Bgl*II-*Hind*III site.

To facilitate detection of the transgene expression within host organs, the luciferase reporter was tagged with 3× FLAG at its N-terminal. Briefly, the fragment of the FLAG-tagged luciferase gene was amplified by polymerase chain reaction (PCR) using forward, 5′-ACCATGGACTACAAAGACCATGACGGTGATTATAAAGATCATGACATCGATTACAAGGATGACGATGACAAGGAAGACGCCAAAAACATAAAG-3′ (the FLAG sequence is inserted between −1 and +1 of luciferase); and reverse, 5′-TTTCGAAGTACTCAGCGTAAG-3′ primers and pGL3-basic as a template. PCR reaction was performed at 95°C for 30 seconds, 55°C for 30 seconds, and 72°C for 45 seconds for 30 cycles, followed by final extension at 72°C for 7 minutes. A fragment of ~240 bp was digested with *Nco*I/*Nsp*V and inserted back into the pGL3 reporter vector at the same site. All sequences were confirmed by dideoxy-DNA sequencing (ABI 377; Applied Biosystems, Foster City, CA).

### Transient Expression Assay

The promoter/enhancer construct that exhibited the best hypoxic inducibility was determined by dual-luciferase assay. Tandem copies of the HRE from the rat VEGF gene cloned 5′ to a hmCMV-promoter-luciferase transcription unit were as described above. Cells were co-transfected (using liposomes) with 500 ng of pHRE-Luc and 25 ng of pRL (Promega) per $1 \times 10^5$ IRPTC in 24-well culture dishes. Transfected cells were exposed to graded hypoxia (1 to 10% $O_2$) for the indicated time and harvested for dual-luciferase assay in fixed protein aliquots. A Lumat 9507 luminometer (EG and Berthold, Bad Wildbad, Germany) was used for measurement. The relative light unit value of the firefly luciferase was divided by that of the renilla luciferase to correct for transfection efficiency.

### Western Blotting and Immunocytochemistry

The temporospatial expression of the target vector (FLAG-tagged luciferase) in IRPTC was confirmed by Western blotting and immunocytochemistry. In Western blotting, whole cell lysates were obtained with RIPA buffer (150 mmol/L NaCl, 1% Nonidet P-40, 0.5% sodium deoxychorate, 0.1% sodium dodecyl sulfate, 50 mmol/L Tris-HCl, pH 8.0), and 40-$\mu$g portions of each were separated by 10% sodium dodecyl sulfate-polyacrylamide gel electrophoresis under reducing conditions. After electrophoresis, samples were transferred to polyvinylidene difluoride membranes (Millipore, Japan). After blocking with 5% skim milk, FLAG-tagged luciferase was developed with mouse monoclonal anti-FLAG (M2) antibody (Sigma) at 1/350 and alkaline phosphatase-conjugated anti-mouse IgG (Promega) at 1/1000. BCIP/NBT tablets (Sigma) were used as a substrate. Coomassie Brilliant Blue (CBB) staining of the membranes confirmed equal loading and transfer. In immunocytochemistry, IRPTCs transfected with the vector plasmid were grown on four-well Lab-Tek chamber slides (Nalge Nunc International, Naperville, IL), fixed with ice-cold methanol/acetone, and stained with anti-FLAG antibody at 1/350, biotinylated anti-mouse IgG (Vector Laboratories, Burlingame, CA) at 1/400 and Oregon Green 488 streptavidin (Molecular Probes, Eugene, OR) at 1/400. Slides were observed with a microscope equipped with fluorescein filters (Olympus, Tokyo, Japan).

### *HRE-Luciferase Transgenic Rats*

Having confirmed pHRE ×7-CMV-Luc as the best hypoxia-responsive vector tested to date, we isolated the transgene by digesting the plasmid at *Kpn*I/*Bam*HI sites, and microinjected the generated 2.4-kbp product into the pronucleus of fertilized eggs of the Wistar in-bred strain. Injected eggs were transferred into the oviduct of pseudopregnant rats. When rats were 3 weeks old, genomic DNA was isolated from the tails and subjected to Southern blotting. The *Bam*HI- or *Pst*I-digested genomic DNA was electrophoresed and blotted onto positively charged nylon membranes (Amersham, Piscataway, NJ) and hybridized with the [$\alpha$-$^{32}$P]-labeled probe, washed to a final stringency of 0.2× SSPE/0.1% sodium dodecyl sulfate at 65°C, and analyzed with a FUJI-BAS 2000 imaging plate (Fuji Film, Tokyo, Japan). The whole length of the transgene labeled by the random-priming method was used as a probe. Transgenic rats were also identified by PCR using Luc-forward, 5′-GCCTACCGTGGTGTTCGTTTCC-3′; and Luc-reverse, 5′-CGCCTCTTTGATTAACGC-CCAG-3′ primers, which generates an amplified fragment of 800 bp. Animals were housed in individual cages in a temperature- and light-controlled environment and allowed free access to chow and water. All experiments were performed in accordance with the guidelines of the Committee on Ethical Animal Care and Use at the University of Tokyo.

### *Real-Time Reverse Transcriptase (RT)-PCR*

The organ distribution and hypoxic inducibility of the transgene were examined by semiquantitative RT-PCR in control (normoxic) and stimulated (cobalt chloride, 30 mg/kg i.p.) rats. RNA of various organs was isolated and reverse-transcribed (ImProm-II Reverse Transcription System; Promega). One-twentieth (v/v) of the cDNA product was used as a template and amplified by PCR for 28 cycles. The fragments were separated on a 2% agarose gel, stained with ethidium bromide, and visualized under UV transillumination. The sets of primers used were Luc-forward, Luc-reverse (above) for luciferase; and $\beta$-actin-forward: 5′-AACCCTAAGGCCAACCGTGAAAAG-3′, and $\beta$-actin-reverse: 5′-TCATGAGGTAGTCTGTCAGGT-3′ for $\beta$-actin, respectively. To further characterize the temporal expression of the transgene within the hypoxic kidney, real-time PCR was performed. Renal cortex was isolated from control and stimulated (cobalt chloride, 30 mg/kg i.p. injection) rats, from which the template cDNA was generated. Using a QuantiTest CYBR Green PCR Kit (Qiagen, Valencia, CA), PCR reactions were performed on an iCycler (Bio-Rad, Hercules, CA) under the following conditions: initial activation at 94°C for 15 minutes, 40 cycles of amplification at 94°C for 15 seconds, 55°C for 30 seconds, and 72°C for 30 seconds. The standard curve method was used to quantify the amount of luciferase mRNA relative to that of $\beta$-actin. Data collection and analysis was performed using iCycler iQ Optical System software (version 3.0a, Bio-Rad). The sets of primers used were Luc-rt-forward: 5′-TCATCGTTGACCGCCTGAAG-3′, and Luc-rt-reverse: 5′-CGTCTTTCCGTGCTCCAAAAC-3′ for luciferase; and $\beta$-actin-rt-forward: 5′-CTTTCTACAATGAGCT-GCGTG-3′, and $\beta$-actin-rt-reverse: 5′-TCATGAGG-TAGTCTGTCAGG-3′ for $\beta$-actin, respectively.

For practical reasons, the up-regulation of the transgene was tested by administering cobalt chloride as a surrogate stimulus for hypoxia throughout the characterization process. The iron chelator desferroxamine or transition metals such as cobalt inhibit prolyl hydroxylation of HIF-1$\alpha$ at residues 564 and/or 402, a step required for binding of von Hippel-Lindau protein and subsequent ubiquitination. Therefore the administration of cobalt stabilizes HIF-1$\alpha$ subunit irrespective of oxygen concentration, with concomitant activation of HIF-1 protein.

### *Ischemia-Reperfusion Injury in the Kidney*

Spatial expression of the transgene in the kidney was characterized by immunohistochemistry. As an experimental model disease best characterized by hypoxia, we took advantage of an ischemia-reperfusion injury in the rat kidney. At day 0, transgenic rats of both genders weighing 300 to 500 g ($n$ = 5) were anesthetized by intraperitoneal administration of ketamine. Body temperature was kept constant at 37°C. Using a midline abdominal incision, left renal arteries and veins were occluded for 45 minutes with microaneurysm clamps. Sham-control rats received only laparotomy, followed by anesthesia. At 0, 1, 2, 4, 8, and 24 hours after clamp release, rats were sacrificed and samples of the kidneys were prepared for histological evaluation.

### *PAN and Remnant Kidney (RK) Models*

Tubulointerstitial hypoxia was further visualized in two distinct models of renal disease: PAN nephrosis and the RK model. PAN nephrosis was induced in 19 female rats weighing 240 to 280 g. At day 0, rats were given a tail vein injection of PAN (Sigma) at 100 mg/kg. At 1 and 2 weeks, kidneys were removed for histological evaluation. The RK model was constructed in 22 male rats (370 to 415 g) in two steps. One week before disease induction, rats received right heminephrectomy under ketamine anesthesia. At day 0 they were again anesthetized and infarction of approximately two-thirds of the left kidney was accomplished by ligation of the posterior and one or two anterior branches of the main renal artery. Histological evaluation was done at 1 and 4 weeks.

A second study consisted of microvasculature studies in the tubulointerstitium. Control, PAN, and RK rats were injected with 1 mg/kg of biotinylated tomato (*Lycopersicon esculentum*) lectin (Vector Laboratories) via tail vein, which binds specifically to vascular endothelial cells in both glomeruli and tubulointerstitium. Precisely 4 minutes later, the kidneys were removed, methyl-Carnoy's fixed, and processed for evaluation. Blood urea nitrogen (BUN) and urinary protein and blood pressure levels were monitored weekly. BUN levels were measured by the urease-indophenol method with Urea N B (Wako), urinary protein by the Bradford method (Bio-Rad), and blood pressure

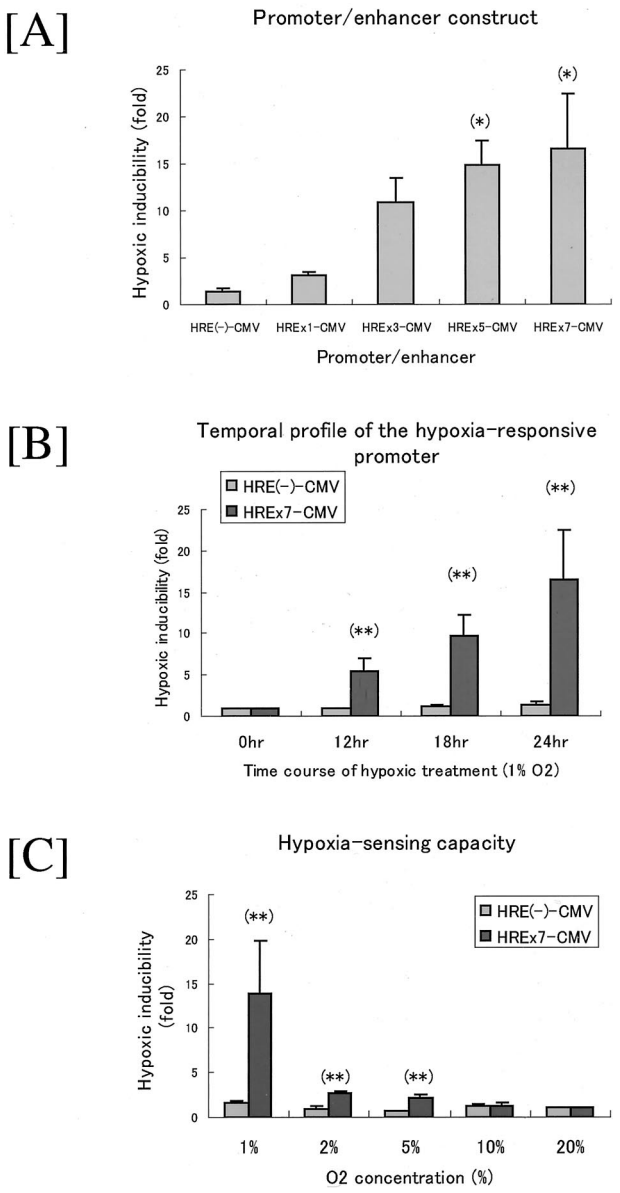


**Figure 1.** Characterization of the hypoxia-responsive vector. FLAG-tagged luciferase reporter vectors driven by HRE (×1, 3, 5, 7 repeats) and hmCMVp were constructed and transfected to IRPTC. **A:** After hypoxic exposure (1% $O_2$, 24 hours), the hypoxic inducibility was calculated as 3.2 ± 0.2-fold, 10.9 ± 2.4-fold, 14.8 ± 2.7-fold ($P < 0.05$), and 16.5 ± 6.8-fold ($P < 0.05$), respectively. Because hypoxic response increased significantly in association with the number of HREs, pHREx7-CMV-Luc was characterized in detail. **B:** Stimulating the transfected cells in 1% $O_2$ for 12, 18, and 24 hours resulted in 5.5-, 9.8-, and 16.5-fold increases in luciferase activity, showing a temporal increase. **C:** The hypoxic response of the reporter was tested in graded oxygen contents. After 24 hours, there was a reciprocal increase in hypoxic inducibility as the oxygen concentration decreased. Statistical significance was reached at less than 5% $O_2$ (dual-luciferase assay; $n \geq 3$; *, $P < 0.05$; **, $P < 0.01$ versus control).

by an occlusive tail-cuff plethysmograph attached to a pneumatic pulse transducer.

## *Histopathology and Immunohistochemistry*

Kidneys were immersion-fixed in methyl-Carnoy's or buffered formalin solutions and embedded in paraffin. Sections (3 $\mu$m) were dewaxed and brought to water through graded alcohols. Periodic acid-Schiff staining was used in light microscopic evaluation for tubulointerstitial injury. Tubulointerstitial injury was assessed semiquantitatively based on morphological changes such as tubular dilatation, atrophy, and thickening of the tubular basement membrane as follows: grade 1, <10% of tubules involved; grade 2, <25%; grade 3, <50%; grade 4, <75%; and grade 5, ≥ 75%, at ×400 magnification in at least 20 consecutive fields in the cortex.

Transgene expression (HRE-driven FLAG-tagged luciferase) was detected by the TSA amplification method (TSA Biotin System; Perkin Elmer, Boston, MA) using anti-FLAG (M2, mouse IgG1) antibody at 1/350. Antigens were developed with $H_2O_2$ and diaminobenzidine (DAB). Negative controls included omission of the incubation step with the primary antibody. Immunohistochemistry for proliferating cell nuclear antigen (PCNA) and ED1 was done by an indirect immunoperoxidase method. Primary antibodies were anti-PCNA (mouse IgG2a; DAKO, Glostrup, Denmark) at 1/500, and anti-ED1 (mouse IgG1; Cymbus Biotechnology, Chandlers Ford, Hants, UK) at 1/40. Terminal dUTP nick-end labeling (TUNEL) staining was performed using a commercially available kit (Trevigen, Gaithersburg, MD).

Double-staining of FLAG (transgene) with PCNA was done using a color modification method of DAB precipitation by nickel chloride, which changes the DAB color from brown to black. Sections were incubated with PCNA followed by biotinylated anti-mouse IgG2a (Santa Cruz Biotechnology, Santa Cruz, CA), horseradish peroxidase-avidin (Vector Laboratories), $H_2O_2$, and nickel chloride containing DAB. Sections were then incubated with anti-FLAG antibody, biotinylated anti-mouse IgG1 (Santa Cruz Biotechnology) and horseradish peroxidase-avidin

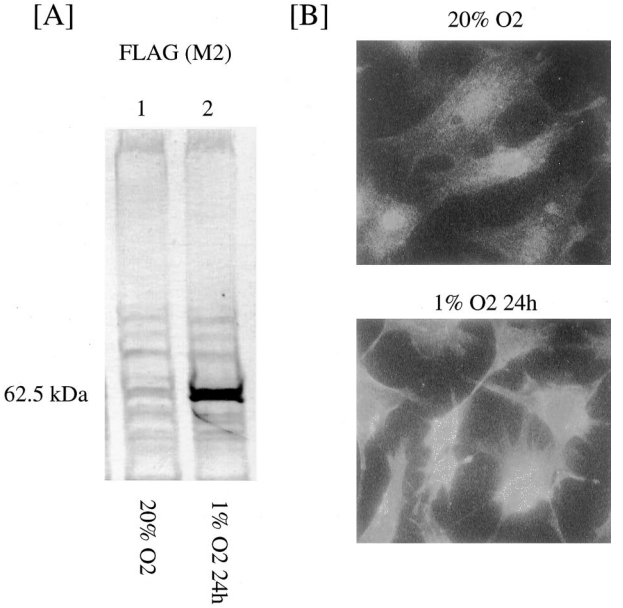


**Figure 2.** Expression of HRE-driven FLAF-tagged luciferase in IRPTC. Expression of FLAG-tagged luciferase was visualized by Western blotting and immunocytochemistry using anti-FLAG (M2) antibody. **A:** In Western blotting, clearly stronger bands were detected at 62.5 kd in hypoxic samples than in controls. **B:** Immunocytochemistry revealed similar hypoxic inducibility of FLAG-tagged luciferase expression within the cytosol.

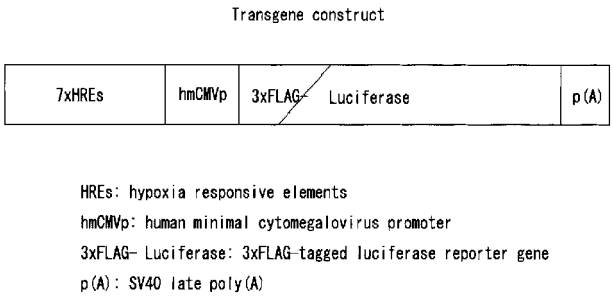


**Figure 3.** Construct of the transgene. A schematic diagram of the transgene is shown. The transgene is controlled by the combination of seven repeats of HRE and hmCMV promoter. To facilitate detection of the transgene expression within the tissues, the luciferase reporter was tagged with 3× FLAG at its N-terminal.

followed by $H_2O_2$ and DAB. Controls included omission of the anti-PCNA antibody and the use of anti-FLAG before anti-PCNA or *vice versa*.

For immunostaining with FLAG and ED1, sections were first stained with ED1 using Ni-DAB, then stripped with glycine-HCl (0.1 mol/L, pH 2.2) for 2 hours with constant stirring and finally reprobed with anti-FLAG antibody. The correlation between hypoxic areas and the number of ED-1-positive cells was obtained by computer image analysis, as previously described,[20] under ×400 magnification. Pictures were taken at three consecutive fields per specimen (RK, 4 weeks, $n = 8$) and the percentage of hypoxic (FLAG-positive) tubular cells was calculated.

### *Statistical Analysis*

Data are expressed as means ± SEM. All analyses were performed using StatView software (version 5.0; SAS Institute, Cary, NC). Differences among groups were compared using the unpaired Student's *t*-test with Bonferroni/Dunn's correction. Nonparametric data were analyzed with the Kruskal-Wallis test when appropriate. *P* values $<0.05$ were considered statistically significant.

## *Results*

### *Establishment of a Hypoxia-Sensing Transgenic Rat*

#### *Development of a Hypoxia-Responsive Reporter Vector*

To construct a hypoxia-responsive vector that senses low partial oxygen concentration and expresses the reporter with maximum activity, we used a 28-bp HRE of the rat VEGF gene located in its 5′ flanking region. FLAG-tagged luciferase reporter vectors under the control of hmCMVp in combination with 1, 3, 5, 7× tandem repeats of HRE were constructed. When transfected to IRPTC and exposed to 1% $O_2$ for 24 hours, the hypoxic inducibility of these plasmids was calculated as 3.2 ± 0.2-fold, 10.9 ± 2.4-fold, 14.8 ± 2.7-fold ($P < 0.05$), and 16.5 ± 6.8-fold ($P < 0.05$), respectively (Figure 1A). The hypoxic response measured as luciferase activity increased significantly as the number of HREs increased, reaching a plateau at the repeat number of 5 through 7.

On this basis result, pHREx7-CMV-Luc was adopted and characterized in detail. Stimulating the vector plasmid in 1% $O_2$ for varying lengths of time, namely 12, 18, and 24 hours, resulted in respective 5.5-, 9.8-, and 16.5-fold increases in luciferase activity, demonstrating a temporal increase in the hypoxia-responsive reporter activity (Figure 1B). Furthermore, when transiently transfected IRPTC was subjected to graded oxygen contents for 24 hours, a reciprocal increase in hypoxic inducibility was seen as oxygen concentration decreased (Figure 1C). A decrease in $O_2$ content to 5% (corresponding to a partial oxygen pressure of 35 to 40 mmHg) resulted in 2.1-fold hypoxic response, which increased thereafter, indicating the ability of this vector plasmid to sense a wide range of hypoxic concentrations. Stimulation of transfected cells with inflammatory cytokines such as tumor necrosis factor-$\alpha$ (recombinant human, 1 to 100 ng/ml) or lipopolysaccharide (1 to 100 $\mu$g/ml) failed to induce any recognizable transcriptional up-regulation (data not shown). Further, a second ubiquitous promoter, thymidine kinase (tk), was additionally tested in place of hmCMVp. Although a similar hypoxic response was seen, the hypoxic inducibility of this promoter was less than that of hmCMVp (data not shown).

The expression of FLAG-tagged luciferase was also visualized by Western blotting and immunocytochemistry using anti-FLAG (M2) antibody (Figure 2). In Western blotting, obvious bands were detected at 62.5 kd in both normoxic and hypoxic samples, but signal intensity was much stronger in the hypoxic samples. Immunocytochemistry revealed similar hypoxic inducibility of FLAG-tagged luciferase expression within the cytosol.

#### *Establishment of Transgenic Rats Carrying the Hypoxia-Responsive Vector*

To establish the hypoxia-sensing transgenic rats, a 2.4-kb vector fragment composed of the FLAG-tagged luciferase gene under the control of 7× HREs was digested and purified. The schematic construct of the transgene is illustrated in Figure 3. The fragment was then microinjected into 200 embryos of the Wistar in-bred strain. Thirteen of fifty-seven putative founders harbored the transgene as confirmed by Southern blotting and PCR of tail DNA. All 13 founder rats expressed the transgene in the kidney, which was confirmed by RT-PCR. The

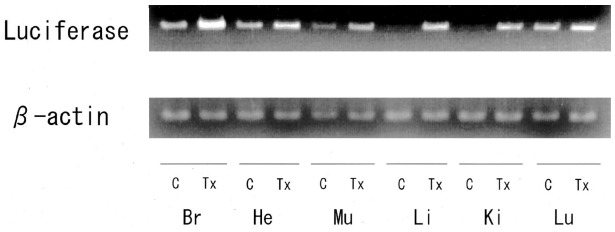


**Figure 4.** Organ distribution of the transgene. Transgene expression in various organs was examined by RT-PCR, both under control and stimulated (cobalt chloride, 30 mg/kg i.p.) conditions. RNA was isolated from brain, heart, muscle, liver, kidney (cortex), and lung. At baseline, the bands of the transgene were faintly visible, but were much stronger in samples of cobalt-treated rats, showing a conditional up-regulation of the transgene (PCR, 26 cycles; representative data).

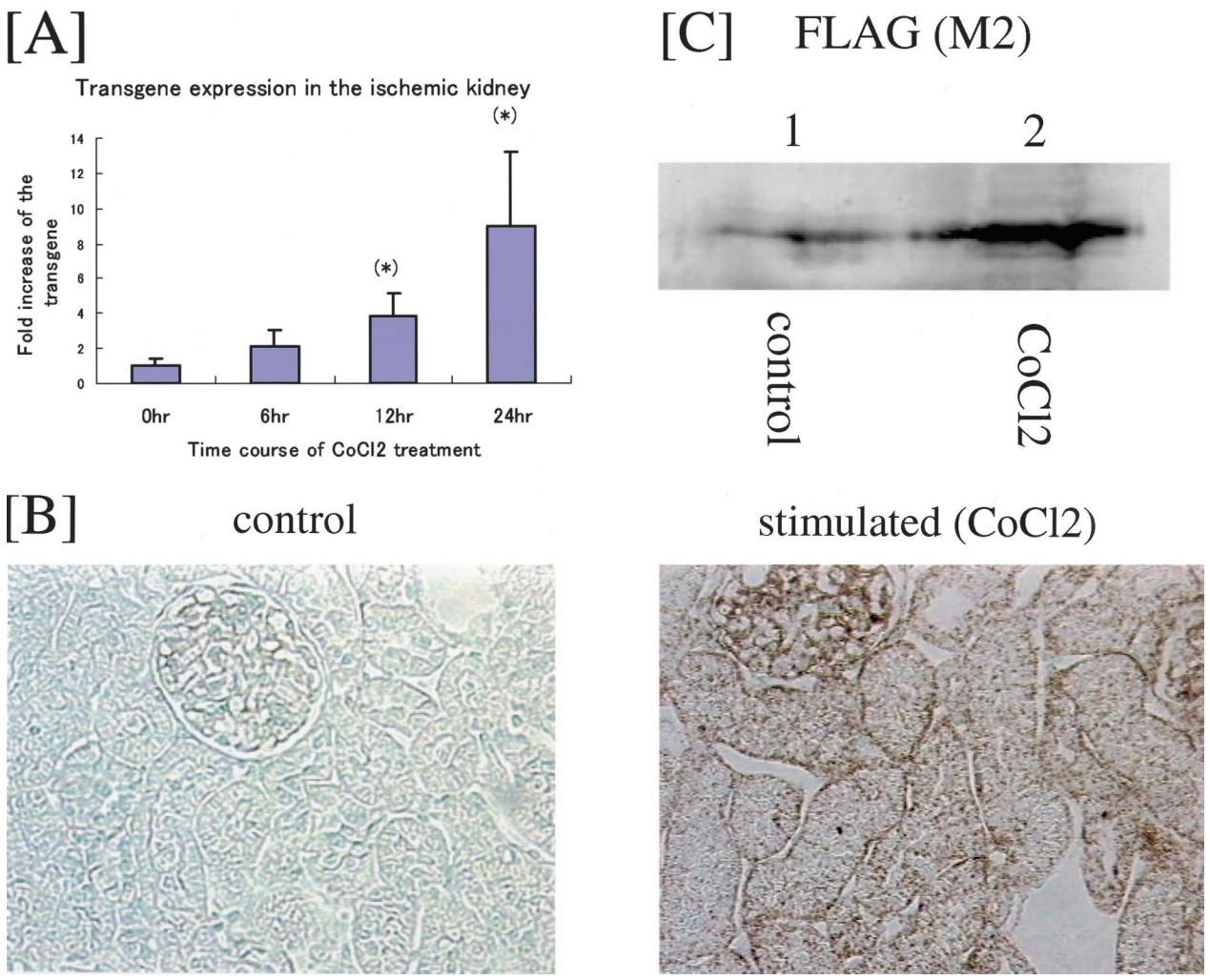


**Figure 5.** Up-regulation of the transgene in the ischemic kidney. Transgene expression was further characterized in the ischemic kidney. **A:** Temporal expression of the transgene in the cortex was measured by real-time PCR. Stimulation with cobalt chloride (30 mg/kg i.p.) for various periods of time caused a temporal increase, reaching 8.9 ± 4.3-fold at 24 hours ($n = 4$; *, $P < 0.05$ versus control). **B:** Spatial expression within the kidney. In control kidneys, the expression of FLAG-tagged luciferase was minimal in the tubulointerstitium. When stimulated with cobalt chloride, expression was markedly increased in tubular cells, glomerular epithelial cells, and interstitial cells. Positive staining was observed in the medullary area in both normoxic and hypoxic samples because of an oxygen gradient within the physiological kidney (not shown). Western blotting in **C** further corroborates quantitative up-regulation of the transgene in response to cobalt stimulation. Aliquots of protein from renal cortex were immunoprecipitated with protein G-Sepharose beads, resolved by 10% sodium dodecyl sulfate-polyacrylamide gel electrophoresis, transferred, and probed with anti-FLAG (M2) antibody. Original magnification, ×400 (**B**).

hypoxic inducibility of the transgene was then tested in these rats using cobalt chloride, a surrogate stimulus for hypoxia. Enhanced transcription of the luciferase gene was seen in only four founders, namely strains no.167-12, no.171-6, no.166-6, and no.173-5. These four founders transmitted the transgene to their progeny at 1:1 Mendelian distribution. General histological examination of various tissues of heterozygous rats revealed no abnormalities throughout development. Further, hematological and biochemical examination of blood samples of transgenic and wild-type rats revealed no apparent difference between them. Subsequent quantitative real-time PCR revealed that the quantitative difference in transgene expression among the founders was no.166-6 > no.171-6 > no.167-12 > no.173-5 (data not shown), which was similar to that in the relative copy number. Because all four strains of transgenic rats exhibited similar characteristics and behaved in the same manner against hypoxic stimulation, we bred and analyzed in detail the two with the higher copy numbers (no.166-6, no.171-6). Results for these two were similar. Heterozygous transgenic rats were used throughout the experiments.

### *Temporospatial Expression of the Transgene*

Transgene expression in various organs was examined by RT-PCR, under both control and stimulated conditions. Cobalt chloride (30 mg/kg) or vehicle (phosphate-buffered saline) was injected intraperitoneally into the rats[21] and RNA was isolated from brain, heart, muscle, liver, kidney (cortex), and lung. RT-PCR analysis revealed that at baseline, the bands of the transgene were faintly visible, whereas in cobalt-treated rats, the bands were obviously stronger than those in controls (Figure 4), showing a conditional up-regulation of the

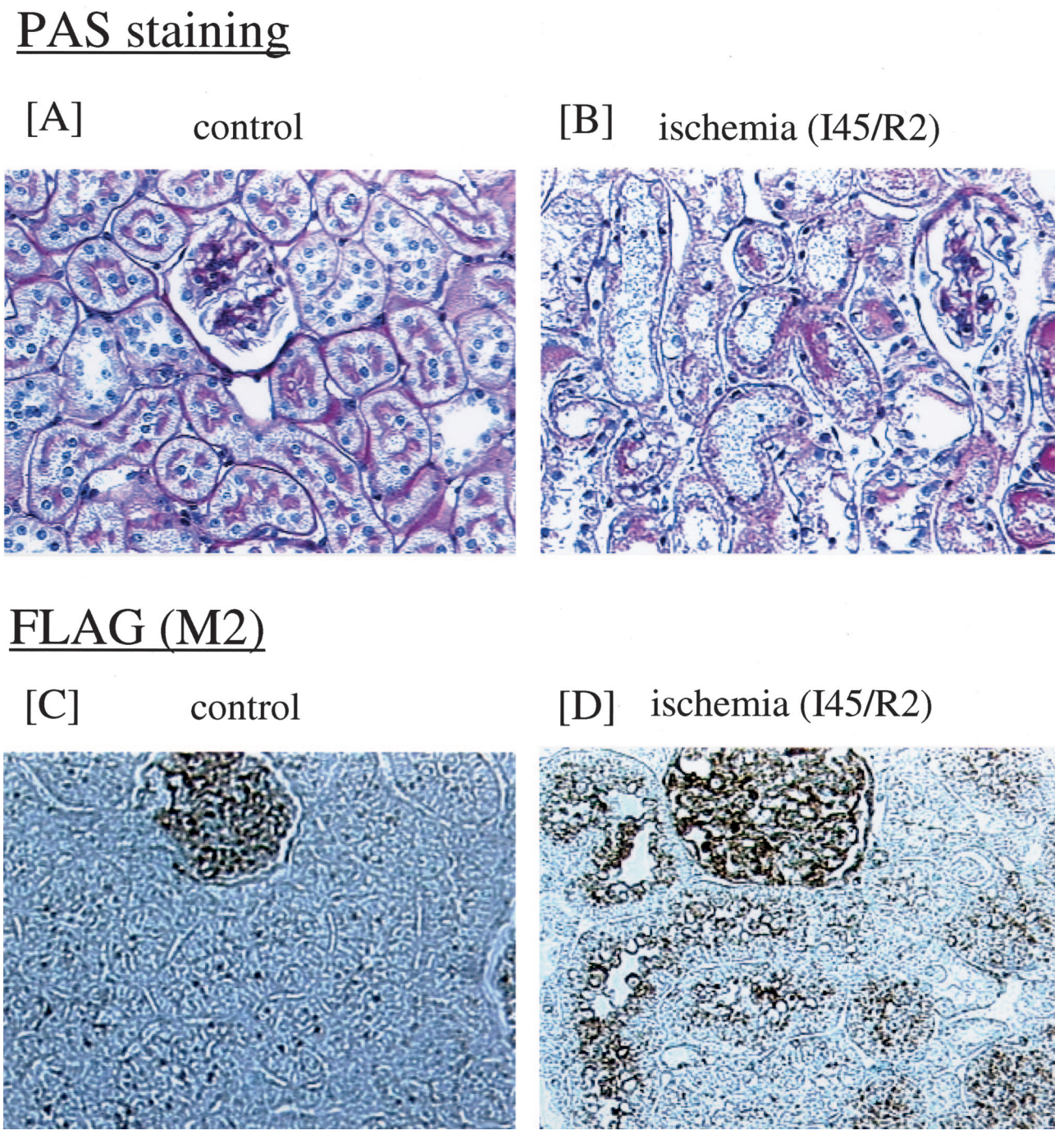


**Figure 6.** Detection of hypoxia in renal ischemia-reperfusion injury. Hypoxia-responsive transgene expression was also verified in the hypoxic, diseased kidney. **A** and **B:** Periodic acid-Schiff staining of the ischemic kidneys revealed morphological changes such as tubular dilatation, sloughing of tubular epithelial cells, cast formation, and interstitial edema. **C** and **D:** Immunostaining with anti-FLAG antibody revealed up-regulation of the transgene in some dilated proximal tubular cells, especially in the apical side 2 hours after reperfusion. Positive staining in proximal tubular cells was observed immediately after clamp-release and persisted for up to 4 hours after reoxygenation (not shown) (ischemia-reperfusion model). Original magnifications, ×400.

transgene. Similar up-regulation of the transgene was observed in immunohistochemistry (not shown).

The temporal expression of the transgene was further characterized in the renal cortex by real-time PCR (Figure 5A). Stimulation of the transgenic rats with cobalt chloride (30 mg/kg i.p.) for varying lengths of time resulted in a clear temporal increase in transgene expression, reaching 8.9 ± 4.3-fold at 24 hours ($P < 0.01$), consistent with our previous *in vitro* experimental results.

The spatial expression of the transgene within the kidney is shown in Figure 5B. In the cortex of control kidneys, the expression of FLAG-tagged luciferase was minimal in both tubular cells and interstitium. On stimulation with cobalt chloride, however, transgene expression was

**Table 1.** General Characteristics of the PAN and RK Models

| | Time course | | | | |
|---|---|---|---|---|---|
| | 0 week | 1 week | 2 weeks | 3 weeks | 4 weeks |
| PAN | | | | | |
| BW (g) | 258 ± 18 | 266 ± 16 | 239 ± 22 | — | — |
| SBP (mmHg) | 133.4 ± 14.6 | 133.3 ± 9.6 | 131.7 ± 12.1 | — | — |
| U-protein (mg/day) | 3.4 ± 0.8 | 690.3 ± 150.1† | 524.8 ± 68.1† | — | — |
| BUN (mg/dl) | 16.5 ± 1.9 | 30.9 ± 11.6† | 25.6 ± 5.4† | — | — |
| RK | | | | | |
| BW (g) | 386 ± 20 | 347 ± 49* | 384 ± 32 | 400 ± 13 | 397 ± 16 |
| SBP (mmHg) | 125.8 ± 14.7 | 151.4 ± 23.4† | 154.3 ± 22.2† | 156.4 ± 13.6† | 166.4 ± 18.2† |
| U-protein (mg/day) | 11.2 ± 5.9 | 7.8 ± 3.6 | 14.2 ± 4.4 | 15.0 ± 8.1 | 57.3 ± 24.4† |
| BUN (mg/dl) | 18.7 ± 4.1 | 31.3 ± 14.6* | 29.7 ± 2.1† | 40.6 ± 13.9† | 54.9 ± 36.1† |

* $P < 0.05$; † $P < 0.01$ *vs* 0 week.
SBP, Systolic blood pressure (mmHg); U-protein, urinary protein.

markedly increased in tubular cells, glomerular epithelial cells, and interstitial cells. Positive staining in mesangial cells was apparently nonspecific, because it was observed even in kidneys of wild-type counterparts (not shown). Also of note was the positive staining of the transgene in the medullary area in both normoxic and hypoxic samples, most likely reflecting the medullary partial oxygen pressure being in the range of 10 to 20 mmHg. Western blotting in Figure 5C further corroborates the up-regulation of the transgene by cobalt stimulation.

### *Up-Regulation of the Transgene in the Ischemic Kidney*

Using our newly developed transgenic rat, we investigated tubulointerstitial hypoxia in ischemia-reperfusion (I/R) injury, a disease model of ischemic acute renal failure. After the left kidney had been cross-clamped for 45 minutes, rats were either processed to renal biopsy or sacrificed for histological evaluation. Periodic acid-Schiff staining of the ischemic kidneys revealed morphological changes such as tubular dilatation, sloughing of tubular epithelial cells, cast formation, and interstitial edema, confirming the adequacy of disease induction (Figure 6, A and B). Immunostaining with anti-FLAG antibody, a marker of tissue hypoxia, was performed. Two hours after clamp release (I45/R2), positive staining was observed in some dilated proximal tubular cells in the ischemic groups, especially in the apical side, as compared to control tissue sections (Figure 6, C and D). Positive staining in proximal tubular cells was observed immediately after clamp release (I45/R0 groups); this staining persisted for up to 4 hours after reoxygenation (I45/R4) and was no longer visible at 8 hours (I45/R8).

## *Tubulointerstitial Hypoxia in Proteinuric Renal Disease and Glomerular Hypertension*

### *General Characteristics*

In the second part, we investigated tubulointerstitial hypoxia in two distinct models of chronic renal disease in rats, PAN-treated experimental nephrotic syndrome (PAN model) and subtotally nephrectomized focal and segmental glomerulosclerosis (RK model). The general characteristics of each disease model are summarized in Table 1. Systolic blood pressure was elevated in the RK model from as early as week 1 until the end of the study [166.4 ± 18.2 mmHg (week 4) versus 125.8 ± 14.7 mmHg (week 0), $P < 0.01$], but remained primarily unchanged in the PAN model. Urinary protein excretion was markedly increased in the PAN model at both 1 and 2 weeks (690.3 ± 150.1 mg/day and 524.8 ± 68.1 mg/day, respectively, $P < 0.01$ versus week 0), whereas proteinuria developed at 4 weeks in the RK model (57.3 ± 24.4 mg/day, $P < 0.01$ versus week 0). BUN levels were mildly elevated from week 1 in both models, and gradually increased thereafter in the RK model (54.9 ± 36.1 mg/dl at week 4, $P < 0.01$ versus week 0).

Histological studies in the cortex of the PAN model revealed markedly dilated tubular cells associated with proteinaceous casts and foci of tubular epithelial disruption, whereas in the glomerulus, no apparent morphological changes were seen. In the RK model, tubules acquired a hypertrophied appearance starting at week 1, and foci of tubular atrophy, dilatation, and interstitial fibrosis developed at week 4, localized mostly in the cortex. Focal changes showing marked mesangial expansion and sclerosis were seen in the glomerulus.

### *Tubulointerstitial Hypoxia*

Tubulointerstitial hypoxia in these models is depicted in Figure 7. In the PAN model, hypoxic tubules were visualized diffusely in the cortex at both 1 and 2 weeks (Figure 7, B, C, and F). In the RK model, on the other hand, hypoxic areas started to extend from the outer medulla to the cortex at week 1, becoming more pronounced at week 4. At this time, foci of atrophic, dilated tubules appeared that exhibited strong signals for the hypoxia-responsive transgene (Figure 7, D, E, and G). A similar distribution of hypoxic areas was identified by pimonidazole staining (not shown). In contrast, immunodetection of VEGF in the cortex revealed comparable staining patterns in control, PAN, and RK groups, which makes a clear contrast to the transgene (not shown). This is an important finding because the transgene expression is controlled by HREs originating from the VEGF promoter. The quantitative data are shown in Figure 7H. The expression of the transgene mRNA in the cortex showed a time-dependent increase in both models, reaching 2.2-fold at 2

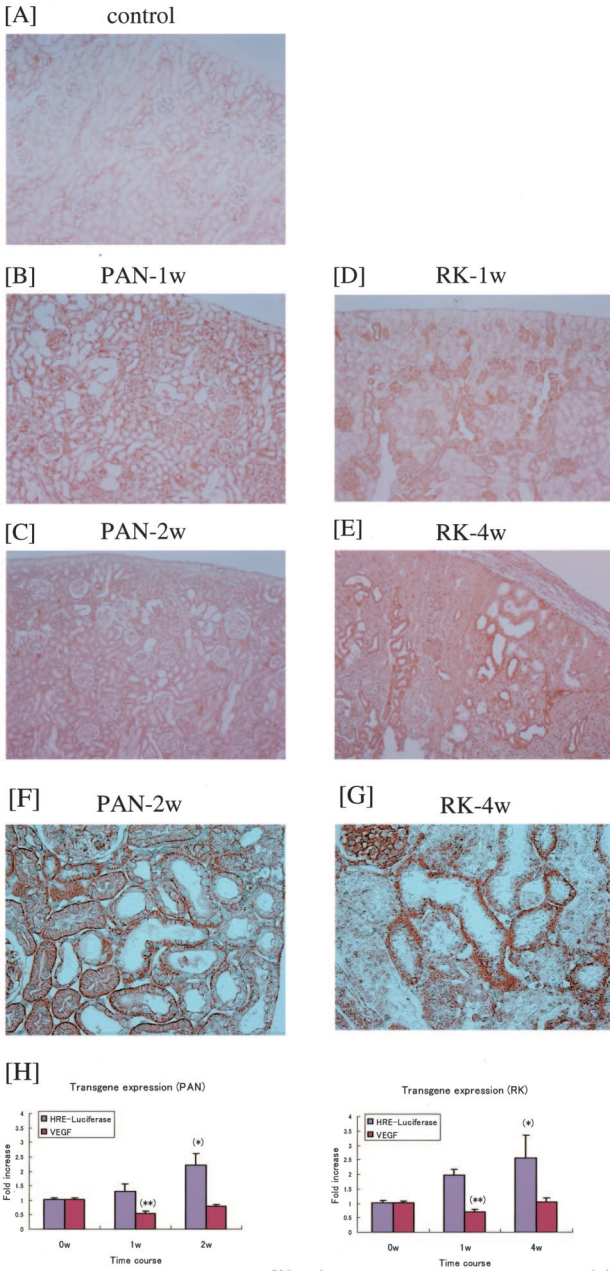


**Figure 7.** Tubular hypoxia in the PAN and RK models. Tubulointerstitial hypoxia is visualized in immunohistochemistry. **B** and **C:** In the PAN model, hypoxic tubules were detected diffusely in the cortex at 1 and 2 weeks. In the RK model, hypoxic areas were essentially focal in the cortex, which extended from the outer medulla to the cortex. **D** and **E:** At 4 weeks, foci of atrophic, dilated tubules appeared exhibiting strong signals for the hypoxia-responsive transgene. **F** and **G:** Representative magnified views in the cortex are shown. In contrast to the diffuse up-regulation in the PAN model, the transgene signal was focal in the RK model, and was especially apparent in dilated, damaged tubules. The quantitative data are shown in **H**. The expression of the transgene mRNA showed a time-dependent increase in both models, reaching 2.2-fold (PAN, 2 weeks) and 2.6-fold (RK, 4 weeks), respectively, whereas VEGF mRNA showed a mild decrease at week 1. Note that they harbor a common responsive element (HRE) in the promoter region (real-time PCR, $n \geq 6$; *, $P < 0.05$; **, $P < 0.01$ versus control). Original magnifications: ×100 (**A–E**); ×400 (**F**, **G**).

weeks in the PAN model and 2.6-fold at 4 weeks in the RK model. VEGF expression, on the other hand, was not significantly altered, or even decreased in the early phase (week 1) in either model, again showing an obviously dis-

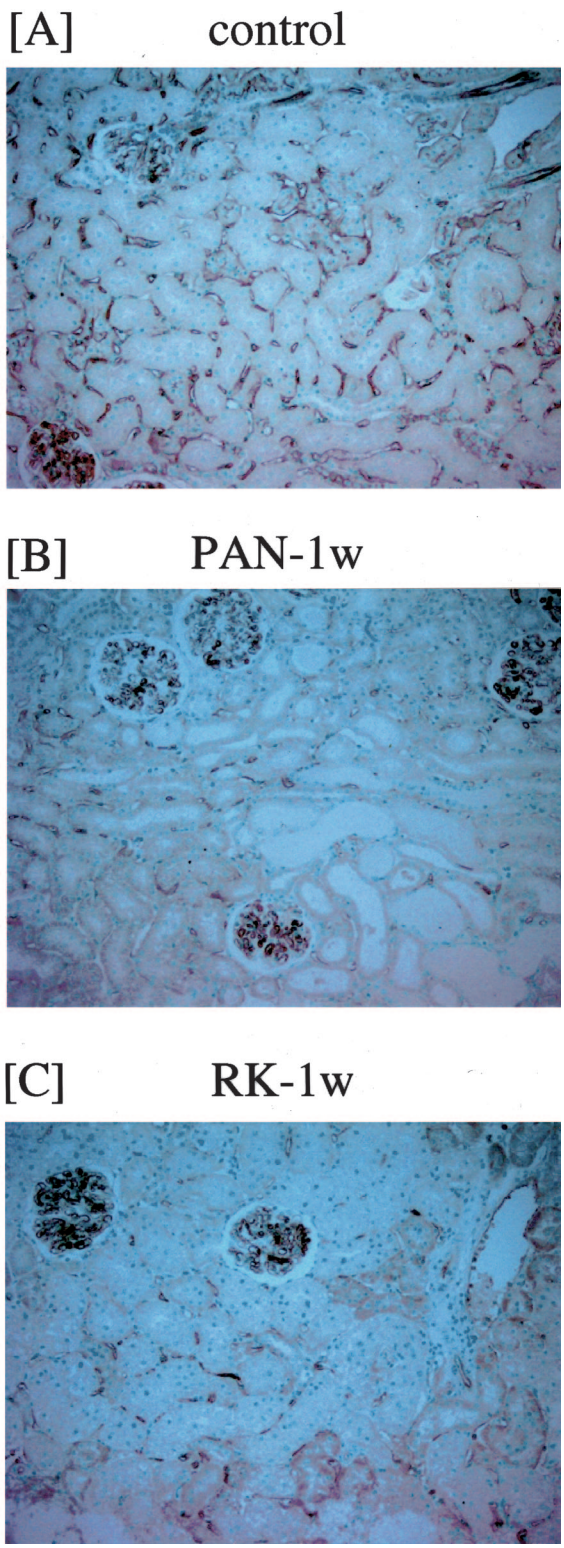


**Figure 8.** Tubulointerstitial microvasculature. Capillary network in the hypoxic tubulointerstitium was examined by tomato lectin perfusion/binding study. In both models, peritubular capillaries were markedly narrowed and disorganized at week 1 (**B** and **C**). The glomerular microvasculature was retained at this stage in both models.

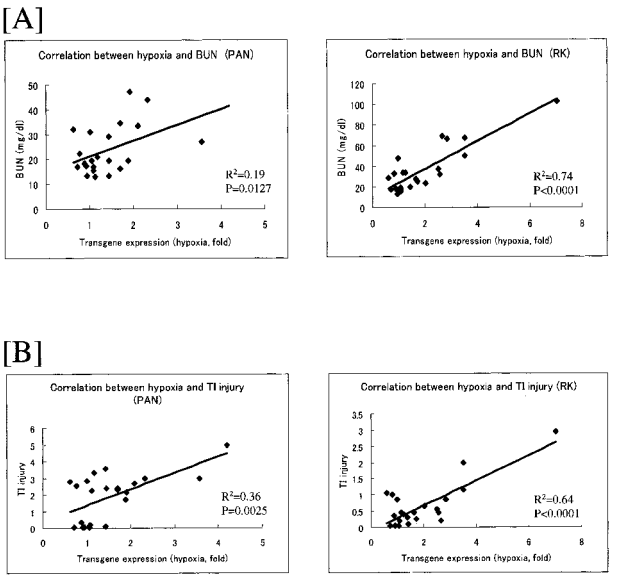


**Figure 9.** Correlation of hypoxia with BUN and tubulointerstitial injury. **A** and **B:** Correlations of hypoxia with BUN and tubulointerstitial injury scores were investigated in individual rats. BUN levels were positively correlated with the degree of hypoxia in both models, with the RK having higher linearity [$R^2 = 0.19$, $P = 0.0127$ (PAN), $R^2 = 0.74$, $P < 0.0001$ (RK)]. Similarly, the extent of tubulointerstitial injury was more highly correlated with hypoxia in the RK model ($R^2 = 0.64$, $P < 0.0001$) than in the PAN-treated rats ($R^2 = 0.36$, $P = 0.0025$).

tinct expression pattern from that of the transgene (HRE-luciferase).

### *Peritubular Microvasculature*

One of the clearest ties found in the literature between regional hypoxia and limited oxygen delivery has been established in impaired peritubular capillaries. For an estimate, we performed a lectin perfusion-binding study (Figure 8). In both models, peritubular capillaries were narrowed and/or distorted at as early as week 1 (Figure 8, B and C). Chronic hypoxia in these models was associated in part with the disorganized network of lectin-binding peritubular endothelial cells.

### *Pathological Involvement/Spatial Co-Localization of the Transgene*

To investigate the possible pathological involvement of tubular hypoxia in these disease models, we examined the correlation of hypoxia with BUN levels and tubulointerstitial injury scores in individual rats (Figure 9, A and B). BUN levels were positively correlated with the degree of hypoxia in both models, with the RK model having higher linearity [$R^2 = 0.19$, $P = 0.0127$ (PAN), $R^2 = 0.74$, $P < 0.0001$ (RK), respectively]. Similarly, the extent of tubulointerstitial injury was found to be more highly correlated with hypoxia among individual rats pooled from week 0 through week 4 in the RK ($R^2 = 0.64$, $P < 0.0001$) than in the PAN rats ($R^2 = 0.36$, $P = 0.0025$).

Finally, we sought to determine the spatial correlation between the transgene and other proteins known to modulate disease progression using the RK model (Figure 10; A to E). Sections were double-stained with anti-FLAG and anti-PCNA (Figure 10A) or anti-ED1 (Figure 10B) antibodies. TUNEL staining was performed in serial sections (Figure 10, C and D). Most of the PCNA-positive tubular cells were positively stained with the transgene in the early (week 1) phase, indicating the proliferation of hypoxic tubular cells (Figure 10A). In the advanced (week 4) stage, macrophage accumulation was observed in areas with hypoxic dilated tubules (Figure 10B). TUNEL-positive, apoptotic cells were surrounded almost exclusively by hypoxic, dilated proximal tubular cells (Figure 10, C and D). The correlation between hypoxic areas and infiltrating macrophages is shown in Figure 10E. A positive correlation was observed ($R^2 = 0.49$, $P < 0.0001$) both spatially and quantitatively, indicating a tendency for macrophages to gather in hypoxic tubulointerstitial areas.

## *Discussion*

In this study, we developed a novel hypoxia-responsive vector using HREs of the rat VEGF gene *in vitro* and generated a transgenic rat that senses tissue hypoxia at the cellular level. The up-regulation of the transgene *in vivo* was confirmed using two distinct methods, cobalt chloride stimulation and ischemia-reperfusion injury in the kidney. As a final step we visualized tubulointerstitial hypoxia in two distinct models of progressive renal disease, PAN-induced experimental nephrotic syndrome and the remnant-kidney model, and gained some insight into the temporospatial relationship of tubular hypoxia with factors known to impact on disease progression.

To date, 2-nitroimidazoles and other nitroaromers such as pimonidazole have been extensively used as markers of hypoxia and in drug targeting in cancer therapy.[22] However, chemical methods such as these are subject to a number of limitations. First, their activity is time-sensitive. The hypoxia probe is metabolized and bound to cells throughout a 1- to 3-hour period, requiring an assumption that the oxygen content, in terms of blood flow to the tissue, remains constant throughout the observation period. Second, they detect hypoxic cells at an oxygen content below 10 mmHg in theory, which is less than that of typical tumor cells.[23–25] True oxygen monitors, like polarographic oxygen sensors, can become noisy and inaccurate, especially at low oxygen levels over relatively large tissue volumes, because their signal is proportional to the measured quantity.

Major advantages of our transgenic rats over previously established methods may be summarized as follows. First, they provide a wide dynamic range of $O_2$ detection. Our hypoxia-responsive transgene works optimally under an oxygen concentration of 1 to 5% (7 to 40 mmHg), as deduced from *in vitro* experiments. The up-regulation of the transgene is relatively quick (within 45 minutes), and the signal disappears quickly once reoxygenation is attained (within 8 hours). The promoter activity is consistent with a direct response to hypoxia because the effect was dependent on the presence of the

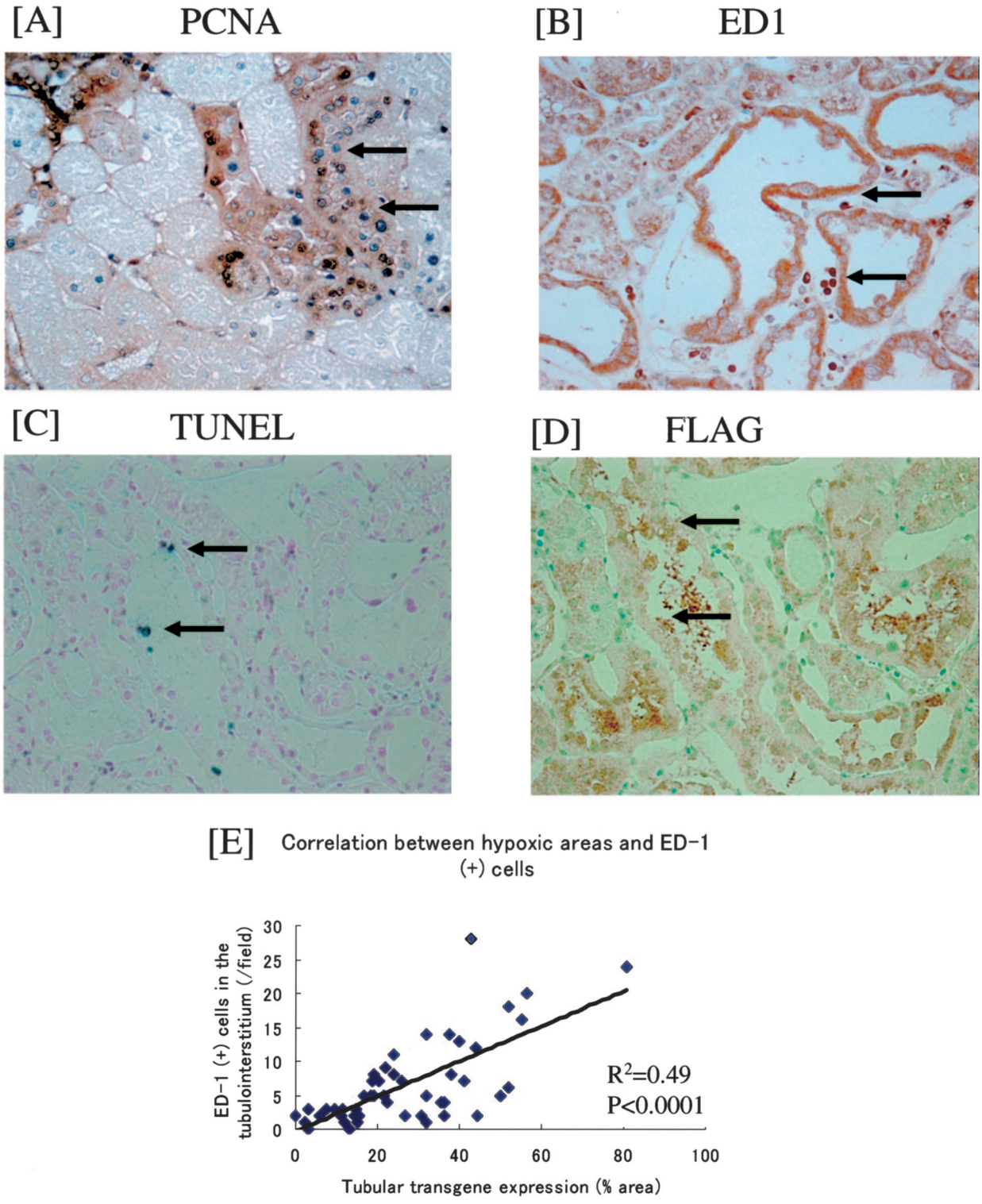


**Figure 10.** Spatial co-localization of the transgene. Spatial co-localization of the transgene with factors modulating disease progression was investigated in the RK model. Sections were double-stained with anti-FLAG and anti-PCNA (**A**) or anti-ED1 (**B**) antibodies. TUNEL staining was performed in serial sections (**C** and **D**). Most PCNA-positive tubules were positively stained with the transgene at 1 week (**A**). At 4 weeks, macrophage accumulation was observed in areas with hypoxic dilated tubules (**B**). Most apoptotic cells were surrounded by hypoxic, dilated proximal tubules (**C** and **D**). Positive cells for PCNA, ED-1, and TUNEL staining are indicated with **arrows**. Correlations between tubular hypoxia and infiltrating macrophages are quantified in **E**. A positive correlation was observed both spatially and quantitatively ($R^2 = 0.49$, $P < 0.0001$). Color development: brown, FLAG; dark brown, PCNA and ED-1; and green, TUNEL. Original magnifications: ×400.

HREs. Second, our transgenic rats allow us to provide information on the relative oxygenation of the tissue mass at a cell-to-cell resolution. Third, the absence of the 3′ untranslated region (UTR) of the rat VEGF gene is also to be noted. VEGF mRNA expression is not only enhanced by HREs at its 5′ flanking region, but also regulated by prolongation of mRNA half-life through posttranscriptional events mediated by specific *cis*-sequences in the 3′ UTR.[26–28] A previous study using the VEGF 5′ promoter[29] had, in fact, predicted information on the areas of hypoxic, yet viable cells. Owing to the internal HIF-HRE system, our transgenic rat is the first *in vivo* biosensor sensing system that allows for automatic quantitative control of transgene expression in response to local hypoxic states.

In the second part of this study, we challenged the hypothesis that tubulointerstitial hypoxia exists and that it plays a pathological role in progressive renal diseases. To address these questions, we adopted two distinct disease models characterized by massive proteinuria and systemic/glomerular hypertension, PAN-induced nephrotic syndrome and subtotally nephrectomized glomerulosclerosis.

Tubulointerstitial injury is a hallmark of progressive renal disease, regardless of the etiology, and chronic hypoxia contributes greatly. Compromise of tubulointerstitial blood flow, directly or through microvascular insufficiency, leads to chronic hypoxia in the tubulointerstitium, which ultimately results in tubular atrophy, leukocyte infiltration, deposition of extracellular matrix, and interstitial fibrosis.[16,17] In support of this hypothesis, administration of angiogenic or vasodilatory factors such as VEGF and NO ameliorates tubulointerstitial damage in a number of glomerular diseases.[30–35] Against it, however, are studies showing negative or contrary results to a role for impaired oxygen content. In one study, for example, higher oxygen tensions were observed in the RK model using needle electrodes.[36] Until now, in fact, direct evidence of reduced oxygen tension in the tubulointerstitium of the diseased kidney has not been available.

The results of the current study clearly show that the renal tubulointerstitium is exposed to hypoxia in the PAN and RK nephropathies. Further, the temporospatial expression of the transgene strongly suggests the pathological involvement of regional hypoxia. The extent of tubulointerstitial hypoxia correlated with the degree of both serum BUN levels and microscopic tubulointerstitial damage. In the RK model, the proliferation of tubular cells was primarily confined to the hypoxic areas, suggesting a high potential for tubular regeneration subsequent to hypoxic injury. Moreover, the presence of macrophages in the hypoxic cortical area was observed; given that macrophages are multifactorial cells capable of synthesizing a number of secretory products that contribute to ongoing tissue injury, their presence here appears to further support the role of hypoxia in the pathogenesis. Furthermore, hypoxia is a strong trigger for apoptosis in cultured renal tubular cells.[37,38] Together, these findings strongly suggest the pathological involvement of regional hypoxia. However, it is also to be noted that overt proteinuria develops and may elicit proinflammatory and profibrotic effects that directly contribute to chronic tubulointerstitial damage.[39]

Regarding renal HIF-1, Rosenberger and colleagues[40,41] recently presented compelling evidence for the operation of this system. Our present study supports and extends their view in that we observed the transcriptional up-regulation of the transgene under the control of HREs in renal tubular cells. Serial sections with FLAG and periodic acid-Schiff staining under control, cobalt-stimulated, and ischemia-reperfusion models have revealed positive staining in distal and proximal tubular cells and cortical collecting ducts of cobalt-treated samples, as well as in proximal tubules with sloughing and cortical collecting ducts of the ischemia-reperfusion group. The tubular structures of transgene expression were basically similar to their observations, except that renal medulla stained positive in all conditions (not shown) and transgene up-regulation was observed also in proximal tubules of Co and I/R groups. The difference of these findings may partly relate to distinct methods we each used. Furthermore, the functional involvement of this system in the diseased kidney has been proposed previously,[42] in which significant improvements of renal histology and function were attained in the rat I/R injury by activating HIF-1 with cobalt chloride.

Microvasculature studies were conducted in an attempt to identify a causal link between regional hypoxia and altered microvascular network. In both the PAN and RK models we investigated here, tubulointerstitial hypoxia was associated with the narrowed and disorganized network of peritubular capillaries, raising the possibility that hypoxia in this compartment was partly induced by impaired blood supply, although much further work is needed to completely clarify this issue because reduced blood supply can only be confirmed by direct measurement of renal blood flow.

Up-regulation of the transgene in the PAN and RK models was rather small, however, as compared with *in vitro* data. The direct interpretation of this is that the tubulointerstitial hypoxia that occurs is very mild. Another possibility left open is that the hypoxic response of the transgene is disproportionately impaired in the diseased kidney, although as yet still oxygen-regulated, as observed in renal Epo transcription.[43,44] It is also to be noted that the disease course of the RK model is so protracted and focal in nature that, although the relative increase in the transgene mRNA is small, it apparently reflects marked overexpression.

Regional hypoxia may either be a trigger that mediates renal pathogenesis or a consequence of tubulointerstitial injury, which are not mutually exclusive. There are, in fact, cases in which tubulointerstitial hypoxia even precedes injury in some immune- and nonimmune-mediated glomerulopathies.[45,46] The findings of such studies may potentially extend the current prevalent view of hypoxia from that of a modulator of tubulointerstitial injury to a possible trigger of it.

Evidence has been accumulating that tissue hypoxia plays a pivotal role in the pathogenesis of various types of human disease, such as stroke, ischemic heart disease, peripheral vascular disease, and solid tumors. Hence the

detection of hypoxia at the cellular level in a highly sensitive way will, in turn, provide new clues to elucidating the pathogenesis as well as a perspective on future therapeutic strategies.

## *Acknowledgments*

We thank Drs. Norio Hanafusa and Takamoto Ohse (University of Tokyo) and Dr. Kiyoshi Kurokawa (Tokai University) for their assistance and advice.

## *References*

1. Wiener CM, Booth G, Semenza GL: In vivo expression of mRNAs encoding hypoxia-inducible factor 1. Biochem Biophys Res Commun 1996, 225:485–488
2. Semenza GL: Regulation of mammalian O2 homeostasis by hypoxia-inducible factor 1. Annu Rev Cell Dev Biol 1999, 15:551–578
3. Semenza GL: HIF-1: mediator of physiological and pathophysiological responses to hypoxia. J Appl Physiol 2000, 88:1474–1480
4. Wenger RH: Mammalian oxygen sensing, signalling and gene regulation. J Exp Biol 2000, 203:1253–1263
5. Jaakkola P, Mole DR, Tian YM, Wilson MI, Gielbert J, Gaskell SJ, Kriegsheim A, Hebestreit HF, Mukherji M, Schofield CJ, Maxwell PH, Pugh CW, Ratcliffe PJ: Targeting of HIF-alpha to the von Hippel-Lindau ubiquitylation complex by O2-regulated prolyl hydroxylation. Science 2001, 292:468–472
6. Ivan M, Kondo K, Yang H, Kim W, Valiando J, Ohh M, Salic A, Asara JM, Lane WS, Kaelin Jr WG: HIFalpha targeted for VHL-mediated destruction by proline hydroxylation: implications for O2 sensing. Science 2001, 292:464–468
7. Yu F, White SB, Zhao Q, Lee FS: HIF-1alpha binding to VHL is regulated by stimulus-sensitive proline hydroxylation. Proc Natl Acad Sci USA 2001, 98:9630–9635
8. Dachs GU, Patterson AV, Firth JD, Ratcliffe PJ, Townsend KM, Stratford IJ, Harris AL: Targeting gene expression to hypoxic tumor cells. Nat Med 1997, 3:515–520
9. Shibata T, Giaccia AJ, Brown JM: Development of a hypoxia-responsive vector for tumor-specific gene therapy. Gene Ther 2000, 7:493–498
10. Prchal JT: Delivery on demand—a new era of gene therapy? N Engl J Med 2003, 348:1282–1283
11. Binley K, Askham Z, Iqball S, Spearman H, Martin L, de Alwis M, Thrasher AJ, Ali RR, Maxwell PH, Kingsman S, Naylor S: Long-term reversal of chronic anemia using a hypoxia-regulated erythropoietin gene therapy. Blood 2002, 100:2406–2413
12. Durand RE, Raleigh JA: Identification of nonproliferating but viable hypoxic tumor cells in vivo. Cancer Res 1998, 58:3547–3550
13. Levy AP, Levy NS, Wegner S, Goldberg MA: Transcriptional regulation of the rat vascular endothelial growth factor gene by hypoxia. J Biol Chem 1995, 270:13333–13340
14. Jacobson HR: Chronic renal failure: pathophysiology. Lancet 1991, 338:419–423
15. Bohle A, Kressel G, Muller CA, Muller GA: The pathogenesis of chronic renal failure. Pathol Res Pract 1989, 185:421–440
16. Fine LG, Bandyopadhay D, Norman JT: Is there a common mechanism for the progression of different types of renal diseases other than proteinuria? Towards the unifying theme of chronic hypoxia. Kidney Int Suppl 2000, 75:S22–S26
17. Fine LG, Orphanides C, Norman JT: Progressive renal disease: the chronic hypoxia hypothesis. Kidney Int Suppl 1998, 65:S74–S78
18. Ingelfinger JR, Jung F, Diamant D, Haveran L, Lee E, Brem A, Tang SS: Rat proximal tubule cell line transformed with origin-defective SV40 DNA: autocrine ANG II feedback. Am J Physiol 1999, 276: F218–F227
19. Boshart M, Weber F, Jahn G, Dorsch-Hasler K, Fleckenstein B, Schaffner W: A very strong enhancer is located upstream of an immediate early gene of human cytomegalovirus. Cell 1985, 41:521–530
20. Kang DH, Joly AH, Oh SW, Hugo C, Kerjaschki D, Gordon KL, Mazzali M, Jefferson JA, Hughes J, Madsen KM, Schreiner GF, Johnson RJ: Impaired angiogenesis in the remnant kidney model: I. Potential role of vascular endothelial growth factor and thrombospondin-1. J Am Soc Nephrol 2001, 12:1434–1447
21. Bergeron M, Gidday JM, Yu AY, Semenza GL, Ferriero DM, Sharp FR: Role of hypoxia-inducible factor-1 in hypoxia-induced ischemic tolerance in neonatal rat brain. Ann Neurol 2000, 48:285–296
22. Chou SC, Flood PM, Raleigh JA: Marking hypoxic cells for complement and cytotoxic T lymphocyte-mediated lysis: using pimonidazole. Br J Cancer Suppl 1996, 27:S213–S216
23. Brizel DM, Sibley GS, Prosnitz LR, Scher RL, Dewhirst MW: Tumor hypoxia adversely affects the prognosis of carcinoma of the head and neck. Int J Radiat Oncol Biol Phys 1997, 38:285–289
24. Hockel M, Knoop C, Schlenger K, Vorndran B, Baussmann E, Mitze M, Knapstein PG, Vaupel P: Intratumoral pO2 predicts survival in advanced cancer of the uterine cervix. Radiother Oncol 1993, 26: 45–50
25. Nordsmark M, Overgaard M, Overgaard J: Pretreatment oxygenation predicts radiation response in advanced squamous cell carcinoma of the head and neck. Radiother Oncol 1996, 41:31–39
26. Shima DT, Deutsch U, D'Amore PA: Hypoxic induction of vascular endothelial growth factor (VEGF) in human epithelial cells is mediated by increases in mRNA stability. FEBS Lett 1995, 370:203–208
27. Levy AP, Levy NS, Goldberg MA: Post-transcriptional regulation of vascular endothelial growth factor by hypoxia. J Biol Chem 1996, 271:2746–2753
28. Damert A, Machein M, Breier G, Fujita MQ, Hanahan D, Risau W, Plate KH: Up-regulation of vascular endothelial growth factor expression in a rat glioma is conferred by two distinct hypoxia-driven mechanisms. Cancer Res 1997, 57:3860–3864
29. Fukumura D, Xavier R, Sugiura T, Chen Y, Park EC, Lu N, Selig M, Nielsen G, Taksir T, Jain RK, Seed B: Tumor induction of VEGF promoter activity in stromal cells. Cell 1998, 94:715–725
30. Masuda Y, Shimizu A, Mori T, Ishiwata T, Kitamura H, Ohashi R, Ishizaki M, Asano G, Sugisaki Y, Yamanaka N: Vascular endothelial growth factor enhances glomerular capillary repair and accelerates resolution of experimentally induced glomerulonephritis. Am J Pathol 2001, 159:599–608
31. Kim YG, Suga SI, Kang DH, Jefferson JA, Mazzali M, Gordon KL, Matsui K, Breiteneder-Geleff S, Shankland SJ, Hughes J, Kerjaschki D, Schreiner GF, Johnson RJ: Vascular endothelial growth factor accelerates renal recovery in experimental thrombotic microangiopathy. Kidney Int 2000, 58:2390–2399
32. Kang DH, Kanellis J, Hugo C, Truong L, Anderson S, Kerjaschki D, Schreiner GF, Johnson RJ: Role of the microvascular endothelium in progressive renal disease. J Am Soc Nephrol 2002, 13:806–816
33. Shao J, Miyata T, Yamada K, Hanafusa N, Wada T, Gordon KL, Inagi R, Kurokawa K, Fujita T, Johnson RJ, Nangaku M: Protective role of nitric oxide in a model of thrombotic microangiopathy in rats. J Am Soc Nephrol 2001, 12:2088–2097
34. Kang DH, Nakagawa T, Feng L, Johnson RJ: Nitric oxide modulates vascular disease in the remnant kidney model. Am J Pathol 2002, 161:239–248
35. Kang DH, Hughes J, Mazzali M, Schreiner GF, Johnson RJ: Impaired angiogenesis in the remnant kidney model: II. Vascular endothelial growth factor administration reduces renal fibrosis and stabilizes renal function. J Am Soc Nephrol 2001, 12:1448–1457
36. Priyadarshi A, Periyasamy S, Burke TJ, Britton SL, Malhotra D, Shapiro JI: Effects of reduction of renal mass on renal oxygen tension and erythropoietin production in the rat. Kidney Int 2002, 61:542–546
37. Saikumar P, Dong Z, Patel Y, Hall K, Hopfer U, Weinberg JM, Venkatachalam MA: Role of hypoxia-induced Bax translocation and cytochrome c release in reoxygenation injury. Oncogene 1998, 17: 3401–3415
38. Tanaka T, Hanafusa N, Ingelfinger JR, Ohse T, Fujita T, Nangaku M: Hypoxia induces apoptosis in SV40-immortalized rat proximal tubular cells through the mitochondrial pathways, devoid of HIF1-mediated upregulation of Bax. Biochem Biophys Res Commun 2003, 309:222–231

39. Eddy AA: Proteinuria and interstitial injury. Nephrol Dial Transplant 2004, 19:277–281
40. Rosenberger C, Mandriota S, Jurgensen JS, Wiesener MS, Horstrup JH, Frei U, Ratcliffe PJ, Maxwell PH, Bachmann S, Eckardt KU: Expression of hypoxia-inducible factor-1alpha and -2alpha in hypoxic and ischemic rat kidneys. J Am Soc Nephrol 2002, 13:1721–1732
41. Rosenberger C, Griethe W, Gruber G, Wiesener M, Frei U, Bachmann S, Eckardt KU: Cellular responses to hypoxia after renal segmental infarction. Kidney Int 2003, 64:874–886
42. Matsumoto M, Makino Y, Tanaka T, Tanaka H, Ishizaka N, Noiri E, Fujita T, Nangaku M: Induction of renoprotective gene expression by cobalt ameliorates ischemic injury of the kidney in rats. J Am Soc Nephrol 2003, 14:1825–1832
43. Tan CC, Eckardt KU, Ratcliffe PJ: Organ distribution of erythropoietin messenger RNA in normal and uremic rats. Kidney Int 1991, 40: 69–76
44. Eckardt KU: Erythropoietin: oxygen-dependent control of erythropoiesis and its failure in renal disease. Nephron 1994, 67:7–23
45. Manotham K, Tanaka T, Matsumoto M, Ohse T, Miyata T, Inagi R, Kurokawa K, Fujita T, Nangaku M: Evidence of tubular hypoxia in the early phase in the remnant kidney model. J Am Soc Nephrol 2004, 15:1277–1288
46. Matsumoto M, Tanaka T, Yamamoto T, Noiri E, Miyata T, Inagi R, Fujita T, Nangaku M: Hypoperfusion of peritubular capillaries induces chronic hypoxia before progression of tubulointerstitial injury in a progressive model of rat glomerulonephritis. J Am Soc Nephrol 2004, 15:1574–1581